

A FLASH PHOTOLYSIS STUDY OF THE PHOTO-OXIDATION OF ACETALDEHYDE AT ROOM TEMPERATURE

R. SIMONAITIS and JULIAN HEICKLEN

Department of Chemistry and Ionosphere Research Laboratory, The Pennsylvania State University, University Park, PA 16802 (U.S.A.)

(Received April 12, 1983; in revised form July 19, 1983)

Summary

Acetaldehyde was flash photolyzed in the presence of air or O₂ at 25 °C. The transient absorption spectrum of CH₃O₂ was monitored and quantum yields were obtained with 310.5, 302.0 and 294.0 nm incident radiation. The CH₃O₂ signal reached full intensity in less than 7 μs, the time resolution of our equipment, at 310.5 nm for a mixture of CH₃CHO at 25.0 Torr and O₂ at 20.0 Torr. The quantum yields decreased with increasing air pressure, the half-quenching pressures being 187 ± 28 Torr, 578 ± 109 Torr and 941 ± 237 Torr respectively for 310.5 nm, 302.0 nm and 294.0 nm incident radiation. These quenching results are in good agreement with values in the literature.

1. Introduction

The photo-oxidation of aldehydes is an important radical source in the atmosphere. In fact in polluted urban atmospheres it may be the main source of radicals which drives the photochemical smog cycle. Therefore it is important to know the radical yields from aldehyde photo-oxidation.

For CH₃CHO there are three possible primary photodecomposition paths:



where A stands for CH₃CHO. In the presence of sufficient O₂, both HCO and H quantitatively give HO₂:



Weaver *et al.* [1] were the first to study the quenching effect of air on process (1b). They measured the CO quantum yield Φ(CO) at 313 nm. Since

reaction (1a) is negligible at 313 nm, reaction (1b) followed by reaction (2) is the sole source of CO, and $\Phi(\text{CO})$ is a direct measure of reaction (1b). They found the CO yield to follow Stern–Volmer quenching with a quenching half-pressure for air of 186 Torr. Thus the CO must come from some precursor which can be removed by collision. This precursor now is believed to be the vibrationally excited triplet state 3A_n [2], so that the competing processes are



Thus $k_4/k_5 = 186$ Torr with 313 nm incident radiation.

This work was extended by Horowitz and Calvert [3] to several incident wavelengths using CO_2 as the quenching gas. To account for the fact that the molecular process (reaction (1a)) occurs at some wavelengths, they measured the yield of $\text{CH}_3 + \text{HCO}$ as $\Phi(\text{CO}) - \Phi(\text{CH}_4)$. Their results are summarized in Table 1. At 313 nm their value for k_4/k_5 is 59 Torr, about one-third that found by Weaver *et al.* [1]. However, Horowitz and Calvert found that CO_2 and CH_3CHO have about the same quenching efficiency, whereas Weaver *et al.* found that CH_3CHO was about three times as efficient a quencher as air. Thus the results of Weaver *et al.* and Horowitz and Calvert are in excellent agreement.

Meyrahn *et al.* [4] measured the primary methyl radical yield (reaction (4)) in 1 atm of air at many wavelengths by measuring the CO and CH_4

TABLE 1

Half-quenching pressure (k_4/k_5) for $\text{CH}_3 + \text{HCO}$ formation in the photo-oxidation of CH_3CHO at 25 °C

λ (nm)	Half-quenching pressure (Torr) from the following sources			
	Weaver <i>et al.</i> [1] ^a	Horowitz and Calvert [3] ^b	Meyrahn <i>et al.</i> [4] ^c	This work ^d
270.0			3448	
290.0		557		
294.0				941 ± 237
300.0		186		
302.0				578 ± 109
304.0			534	
310.5				187 ± 28
313.0	186	59	286	
		52		
320.0		43		
331.2		43		

^a Quenching gas, air.

^b Quenching gas, CH_3CHO .

^c Quenching gas, air.

^d Quenching gas, air; uncertainties represent one standard deviation.

yields. However, they had a sensitive technique whereby they could study air mixtures containing only about 100 ppm CH_3CHO rather than the 10 - 15 Torr used by Weaver *et al.* and Horowitz and Calvert. Pressure quenching experiments were done at three wavelengths, and the half-quenching pressures (k_4/k_5) are given in Table 1. At 313 nm, their value for k_4/k_5 is about 50% larger than that found by Weaver *et al.* In the experiments both of Horowitz and Calvert and of Meyrahn *et al.* the quenching half-pressure increases with incident energy, as expected since k_4 should increase with energy.

All the above-described experiments were done using static steady state photolysis and measuring $\Phi(\text{CO})$ and $\Phi(\text{CH}_4)$ after termination of the radiation. Flash photolysis experiments were performed by Gill and Atkinson [5] and Gill *et al.* [6]. They measured the $\text{HCO}(0,0,0)$ yields (in the absence of O_2) by kinetic spectroscopy and found a 100 - 250 μs delay (depending on the incident wavelength) in its appearance after excitation. This delay time is much longer than that for any possible precursor state of CH_3CHO . Thus the investigators interpreted their results by proposing that reaction (1c) was the exclusive primary radical process and that HCO must be formed in secondary reactions.

To check the above hypothesis, Horowitz *et al.* [2] measured the efficiencies of the various processes with 300 nm radiation using steady state photolysis. They found the limiting low pressure yields to be $\phi_{1a} \approx 0.01$, $\phi_{1b} \approx 0.93$ and $\phi_{1c} \approx 0.06$. Similar results were found at 290, 300 and 313 nm by Horowitz and Calvert [3], with the CH_3CO yield dropping to zero above 320 nm. Thus a discrepancy exists between the static steady state photolysis and the flash photolysis results.

In order to investigate the possible cause of this discrepancy further, we have undertaken a study of the laser flash photolysis of CH_3CHO in the presence of O_2 or air and have measured the CH_3O_2 radical yield which is produced via



Thus our method should provide a direct measure for primary process (1b).

2. Experimental details

CH_3CHO (11 - 25 Torr) was photolyzed with a frequency-doubled dye laser at 294.0, 302.0 and 310.1 nm (the uncertainty in the wavelength measurement is ± 0.3 nm) in the presence of air at 30 - 700 Torr. The transient absorption at 250.5 nm was measured with a limiting time constant of 7 μs or more. The arrangement of the apparatus is shown in Fig. 1. The red laser beam (approximately 1 cm in diameter) from a Phase-R DL 1100 laser is focused by a quartz lens of 55 cm focal length onto a Phase-R AD-ATP crystal frequency doubler. After having its frequency doubled, the beam passes through a Corning 7-54 filter to remove the residual red light. Another

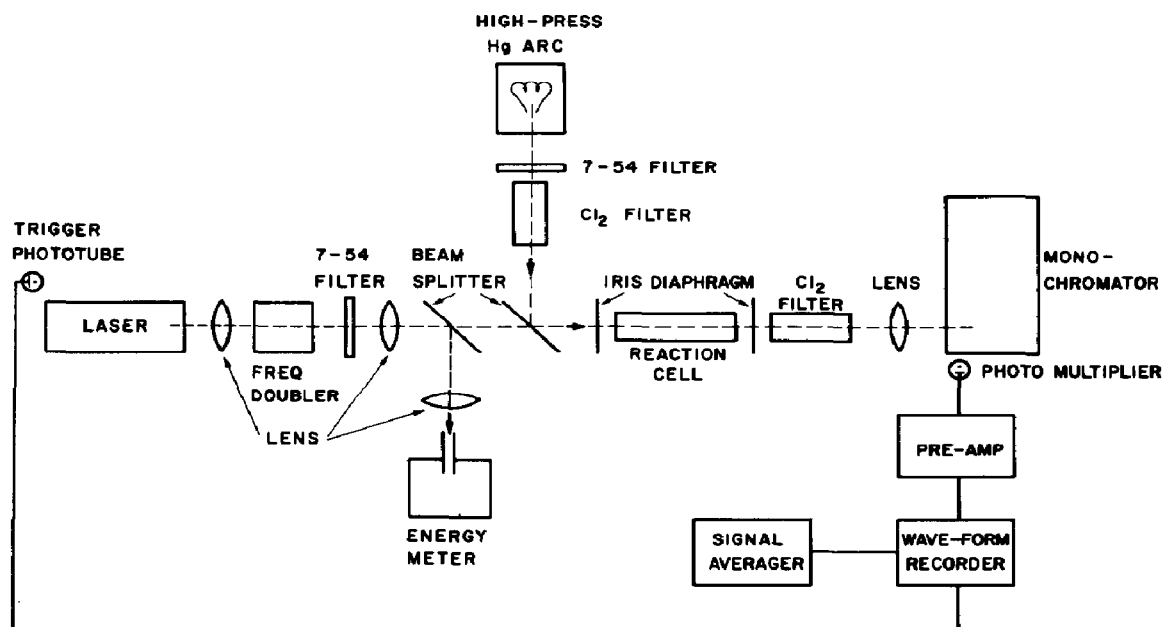


Fig. 1. Schematic diagram of the optical system.

quartz lens of 55 cm focal length defocuses the beam, which then passes through two quartz plate beam splitters and an iris diaphragm before entering the reaction cell. The first beam splitter diverts about 5% of the energy through a focusing lens onto a Laser Precision Corporation Rj-7100 energy meter to monitor the flash intensity. The second beam splitter passes about 95% of the laser light and is used to reflect the monitoring light into the cell.

The monitoring light is a 100 W high pressure mercury arc from TJ Sales Associates, lamp type 100-1083. It passes through Corning 7-54 and Cl_2 filters to isolate the partially reversed 253.7 nm mercury line. The monitoring beam is then reflected by the quartz plate and enters the reaction cell coaxially with the laser beam.

The cylindrical reaction cell is Pyrex with quartz windows. It is 49 cm long and 2.7 cm in diameter. After exiting the cell the laser and monitoring beams pass through an iris diaphragm and a Cl_2 filter to remove the laser light. The remaining monitoring light is focused by a lens onto the entrance slit of a Bausch and Lomb 33-86-49 monochromator which passes the monitoring light centered at 250.5 nm (the maximum of one of the wings of the reversed 253.7 nm line). Both entrance and exit slits of the monochromator are set at 5.0 mm, so that the bandpass is 8 nm.

After exiting the monochromator, the analysis beam impinges on a Hamamatsu 1P28 photomultiplier. The photomultiplier signal is amplified with a home-made differential pulse amplifier and recorded on a Biomation 805 waveform recorder. The recorder is triggered by the laser pulse, a fraction of which has impinged on a trigger phototube (RCA 935). In order to

TABLE 2

Absorption cross sections σ for CH_3CHO and Cl_2 at 25 °C

λ (nm)	$10^{20}\sigma$ (cm ²) ^a	$10^{20}\sigma$ (cm ²) ^b
<i>CH₃CHO</i>		
290.0		4.52
294.0	4.3 ± 0.4	
300.0		3.86
302.0	3.2 ± 0.3	
310.5	2.1 ± 0.2	
313.0	1.9 ± 0.2	2.37
320.0		1.43
331.2		0.37
<i>Cl₂</i>		
294.0		8.4
302.0		13.4
310.5	18.8	18.6

^a This work; band halfwidth, 8 nm.

^b Values for CH_3CHO from Horowitz and Calvert [3]; values for Cl_2 from DeMore *et al.* [7].

improve the signal-to-noise ratio, 10 - 200 laser shots are averaged with a Tracor Northern Digital signal averager NS-570.

Actinometry for quantum yield determinations was done by photolyzing optically equivalent mixtures of $\text{Cl}_2\text{-O}_2\text{-CH}_4$ or $\text{Cl}_2\text{-O}_2\text{-C}_2\text{H}_6$ (Cl_2 at about 5 Torr in O_2 at about 50 Torr containing about 5% hydrocarbon). The extinction coefficients used for CH_3CHO were those measured by us, while those used for Cl_2 were from ref. 7. They are listed in Table 2 together with values from the literature. The photolysis of the $\text{Cl}_2\text{-O}_2\text{-CH}_4$ mixture provides the CH_3O_2 radical with a quantum yield of 2.0. For some runs $\text{Cl}_2\text{-O}_2\text{-C}_2\text{H}_6$ mixtures were used to be sure that any possible impurities in the $\text{Cl}_2\text{-O}_2\text{-CH}_4$ were not scavenging some of the chlorine atoms, since the reactivity of Cl with CH_4 is relatively low. This mixture gives $\text{C}_2\text{H}_5\text{O}_2$ radicals, but the results for both actinometers were identical. This suggests that the absorption cross sections are identical for CH_3O_2 and $\text{C}_2\text{H}_5\text{O}_2$. Values in the literature for these cross sections are given in Table 3. Spectra of both CH_3O_2 and $\text{C}_2\text{H}_5\text{O}_2$ were taken by Adachi *et al.* [8, 9]. They found that CH_3O_2 is a stronger absorber (by a factor of 1.56 at 250 nm). However, other investigators [10, 11] found absorption cross sections for CH_3O_2 lower than that reported by Adachi *et al.* [9] and more in line with the value reported for $\text{C}_2\text{H}_5\text{O}_2$ [8]. Since we found the same results with CH_3O_2 and $\text{C}_2\text{H}_5\text{O}_2$, we assume them to have the same absorption cross section. If this assumption is erroneous, it will alter our absolute quantum yields but will not affect our quenching constants.

TABLE 3

Absorption cross sections σ for RO₂ radicals at 25 °C

λ (nm)	$10^{20} \sigma$ (cm ²) for the following radicals						
	$C_2H_5O_2^a$	$CH_3O_2^b$	$CH_3O_2^c$	$CH_3O_2^d$	HO_2^e	HO_2^f	HO_2^g
210.0				161	669	445	420
212.5		363					
215.0		363				415	
220.0	215	382	317	260	575	370	350
225.0	295	486				285	
227.5	310						
230.0	347	486	413	317	384	230	230
232.5	372						
235.0	389	574				160	
237.5	387						
240.0	367	593	432	317	191	80	120
242.5	345						
245.0	332	574				20	
247.5	336						
250.0	316	493	390	268	71		47
252.5	293						
255	286	440					
260	248	379	306	210	19		
265	203	333					
270	167	306	191	145			
275	130	218					
280	104	146	80	76			

^a From Adachi *et al.* [8].^b From Adachi *et al.* [9].^c From Parkes *et al.* [10].^d From Hochanadel *et al.* [11].^e From Hochanadel *et al.* [12].^f From Paukert and Johnston [13].^g From Cox and Burrows [14].

CH₃CHO (Aldrich, 99%) was degassed at -196 °C and used without further purification. Cl₂ (Matheson, research grade) was passed over KOH to remove HCl and degassed at -196 °C. Its UV absorption spectrum indicated a purity of 95% or more. The CH₄ (Matheson, ultrahigh purity) and the C₂H₆ (Matheson, CP grade) were used directly from the cylinder. Laboratory air was used after being dried by rapid passage through a trap at -196 °C. All gases were handled in a conventional glass vacuum line containing Teflon stopcocks with Viton O-rings. The Cl₂ pressure was measured on an H₂SO₄ manometer, the CH₃CHO pressure on a Wallace and Tiernan model FA-160 0 - 50 Torr absolute pressure indicator and the air on a calibrated NRC 820 alphanatron gauge.

3. Results and discussion

When $\text{CH}_3\text{CHO}-\text{O}_2$ or the actinometer mixtures are flash photolyzed with the laser, a transient absorption is seen at 250.5 nm. Pictures of these absorptions are given in Figs. 2 and 3. Shortly after the flash, the absorption appears and remains constant for many microseconds. If we attribute this absorption solely to CH_3O_2 , then quantum yields Φ of CH_3O_2 can be computed. These values are listed in Table 4 as a function of air pressure and incident wavelength λ . The quantum yields decrease as the pressure is raised at each wavelength.

Actually, the absorption is not due solely to CH_3O_2 . If process (1c) occurs, then $\text{CH}_3\text{C}(\text{O})\text{O}_2$ will also be present. Horowitz and Calvert [3] showed that the quantum yield for process (1c) is 0.065 ± 0.01 between 290 and 313 nm. Thus the error introduced by neglecting this process should be small. Moreover, if the absorption coefficient for $\text{CH}_3\text{C}(\text{O})\text{O}_2$ is similar to that for CH_3O_2 , then we are measuring the sum of the yields for processes (1b) and (1c).

A more serious error in the quantum yield measurements arises from the fact that HO_2 also absorbs at 250 nm. Since every CH_3O_2 (and $\text{CH}_3\text{C}(\text{O})\text{O}_2$) is formed along with one HO_2 radical, the HO_2 absorption must be included in the calculation to obtain accurate quantum yields, although the quenching coefficient will be unaffected whether or not the HO_2 correction is included. Extinction coefficients for CH_3O_2 and HO_2 are listed in Table 3. At 250 nm $\sigma(\text{CH}_3\text{O}_2) = (3.8 \pm 1.1) \times 10^{-18} \text{ cm}^2$ and $\sigma(\text{HO}_2) =$

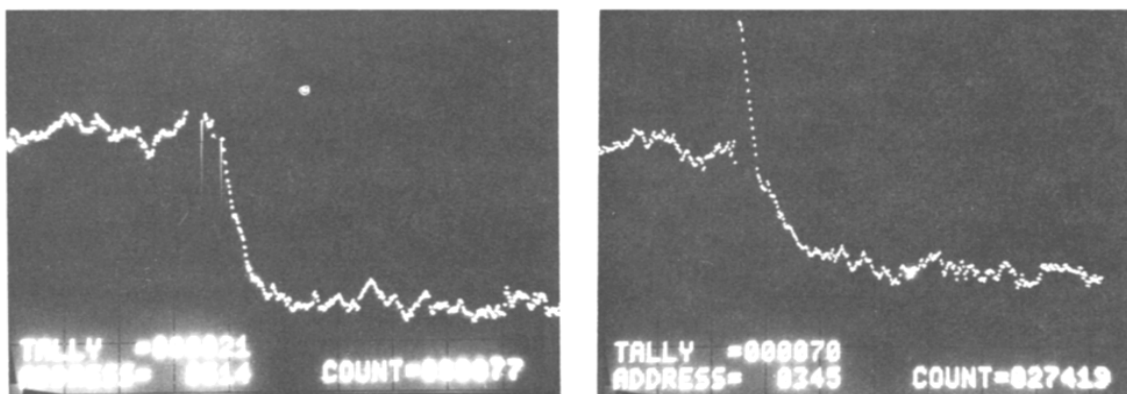


Fig. 2. Plot of light intensity at 250.5 nm vs. time after the flash in the 310.5 nm photolysis of a mixture containing Cl_2 at 3.4 Torr, C_2H_6 at about 2.5 Torr and excess O_2 to bring the total pressure to 54.0 Torr. The time scale runs from left to right with a sweep time of $2 \mu\text{s}$ per channel. The fraction of light absorbed is 0.0045. The plot is an average of 21 shots.

Fig. 3. Plot of light intensity at 250.5 nm vs. time after the flash in the 310.5 nm photolysis of a mixture of CH_3CHO at 24 Torr and O_2 at 16 Torr. The time scale runs from left to right with a sweep time of $2 \mu\text{s}$ per channel. The fraction of light absorbed is 0.0021. The plot is an average of 70 shots.

TABLE 4

Photolysis of CH_3CHO in the presence of air: quantum yields for CH_3O_2 formation

Total pressure (Torr)	\bar{E}^a	N^b	Φ
$\lambda = 310.5 \pm 0.3 \text{ nm}; \text{CH}_3\text{CHO}$ at 20.0 Torr			
38.0 ^c	0.47	20	0.87
38.0 ^c	0.42	20	1.00
38.2 ^c	0.41	30	1.17
38.2 ^c	0.52	20	1.07
40 ^d	0.37	70	1.06
45.0 ^{c,e}	0.53	100	0.98
166	0.33	30	0.70
166	0.30	40	0.66
305	0.38	40	0.50
305	0.36	40	0.51
360	0.37	40	0.60
484	0.38	80	0.40
520 ^e	0.42	199	0.33
$\lambda = 302.0 \pm 0.3 \text{ nm}; \text{CH}_3\text{CHO}$ at 11.0 Torr			
18 ^c	0.33	30	1.35
18 ^c	0.54	30	1.09
35.0 ^c	0.40	30	1.02
38.0 ^c	0.37	40	1.25
38.0 ^c	0.39	30	1.27
111	0.45	40	1.16
111	0.53	38	1.06
111	0.54	40	1.30
138	0.42	30	1.03
169	0.56	40	0.99
240	0.48	30	1.04
240	0.48	30	0.76
305	0.45	30	0.98
305	0.50	30	1.02
305	0.43	32	0.89
388	0.57	40	0.88
388	0.63	40	0.82
498	0.48	30	0.59
$\lambda = 294.0 \pm 0.3 \text{ nm}; \text{CH}_3\text{CHO}$ at 11.0 Torr			
36.0 ^c	0.66	31	1.29
43.2 ^c	0.82	20	1.09
52.7 ^c	0.66	10	1.18
110	1.23	20	1.06
277	0.51	30	1.28
291	0.64	20	0.93
291	0.60	20	1.19
388	1.21	20	1.10
388	1.24	10	1.04
388	1.17	11	0.96
623	0.74	10	0.73
623	0.74	10	0.73

^a Average relative energy per shot.

^b Number of laser shots.

^c $\text{CH}_3\text{CHO} + \text{O}_2$ only.

^d CH_3CHO at 24.0 Torr.

^e CH_3CHO at 25.0 Torr.

$(0.35 \pm 0.35) \times 10^{-18} \text{ cm}^2$. Thus HO_2 accounts for about 9% of the total absorption. Consequently the quantum yields Φ listed in Table 4 represent approximately $1.09 (\phi_{1b} + \phi_{1c})$.

The mechanism consisting of reactions (4) and (5) leads to the rate law

$$\Phi_0(\text{CH}_3\text{O}_2)\Phi(\text{CH}_3\text{O}_2)^{-1} = 1 + k_5[\text{M}]/k_4 \quad (7)$$

where $[\text{M}]$ is the effective total pressure and $\Phi_0(\text{CH}_3\text{O}_2)$ is the zero-pressure quantum yield of CH_3O_2 . If we incorporate the corrections for $\text{CH}_3\text{C}(\text{O})\text{O}_2$ and HO_2 and realize that at zero pressure the sum of the $\text{CH}_3\text{C}(\text{O})\text{O}_2$ and CH_3O_2 yields is approximately 0.98 between 294 and 310 nm [3] then

$$\Phi^{-1} = (0.93 \pm 0.09)(1 + k_5[\text{M}]/k_4) \quad (8)$$

Figure 4 shows plots of Φ^{-1} versus $[\text{M}]$ for the three wavelengths studied. The values for $[\text{M}]$ are computed as $[\text{air}] + 3[\text{CH}_3\text{CHO}]$ to conform to the relative quenching efficiencies reported by Weaver *et al.* [1]. The straight lines represent the least-squares fit. The intercepts are 0.74 ± 0.07 at 294.0 and 302.0 nm and 0.67 ± 0.09 at 310.5 nm, where the uncertainties represent one standard deviation. These are lower than the expected value of 0.93, and suggest that either the correction for HO_2 absorption should have been larger or the actinometry is about 20% in error. Nevertheless, the ratio of slope to intercept is independent of these errors and gives values of $k_4/k_5 = 941 \pm 237$ Torr, 578 ± 109 Torr and 187 ± 28 Torr respectively at

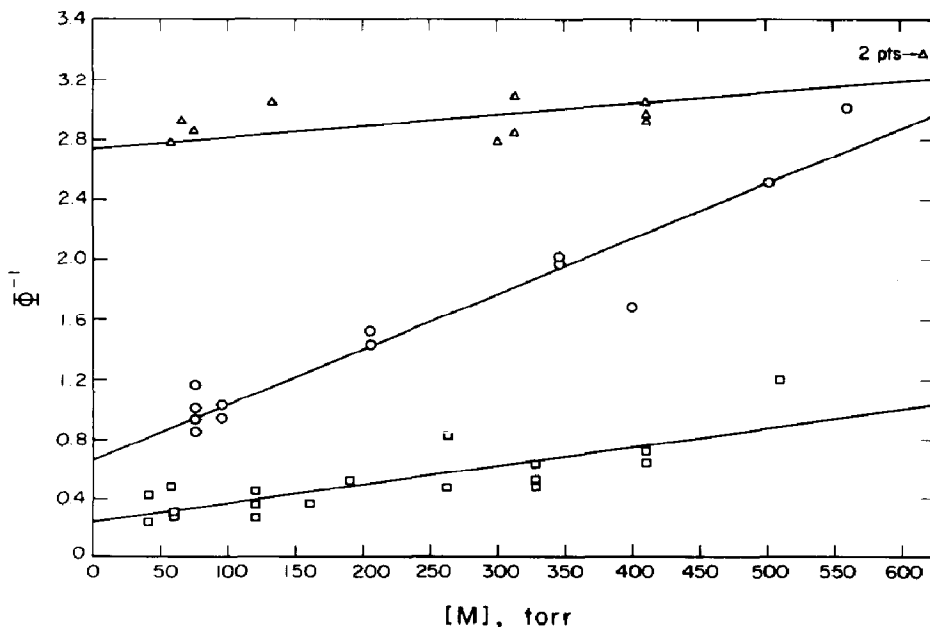


Fig. 4. Plots of Φ^{-1} vs. $[\text{M}]$ where $[\text{M}] = [\text{air}] + 3[\text{CH}_3\text{CHO}]$: \circ , 310.5 nm; \square , 302.0 nm; \triangle , 294.0 nm. The data at 302.0 nm have been displaced downward by 0.5, and those at 294.0 nm have been displaced upward by 2.0 for clarity.

294.0 nm, 302.0 nm and 310.5 nm. These values are in excellent agreement with the values of Weaver *et al.* [1] and Meyrahn *et al.* [4]. The only discrepancy is near 310 nm, where Meyrahn *et al.* [4] obtain values for k_4/k_5 about 50% larger than the values of other investigators. Also included in Table 1 are the half-quenching pressures found by Horowitz and Calvert [3] based on CH_3CHO as a quenching gas. These values are in excellent agreement with ours based on the relative quenching efficiency for CH_3CHO compared with air of 3.0 reported by Weaver *et al.* [1]. If the relative quenching efficiency of 2.4 reported by Horowitz and Calvert [3] is used, the agreement is not quite as good, but still satisfactory.

In order to obtain the lifetime for formation of the CH_3O_2 radical, we increased our detection time resolution from our usual operating condition of 2 μs per channel to 0.8 μs per channel. This reduced our limit for lifetime measurements from about 20 to 7 μs . A plot of the absorption in such an experiment is shown in Fig. 5 for incident radiation at 310.5 nm for a mixture of CH_3CHO at 25.0 Torr and O_2 at 20.0 Torr. The CH_3O_2 signal rose to its maximum with a lifetime of about 7 μs , the limit of our instrument resolution. This time is very much smaller than the values of 100 - 250 μs found by Gill and Atkinson [5] and Gill *et al.* [6] for the HCO formation time. We do not understand their long delay times. From our results, we conclude that the delay time for radical formation is less than 7 μs and that the radicals arise directly from a primary photodissociation process.

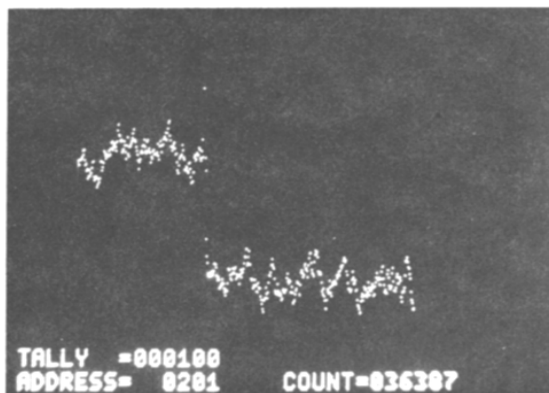


Fig. 5. Plot of light intensity at 250.5 nm vs. time after the flash in the photolysis of a mixture of CH_3CHO at 25.0 Torr and O_2 at 20.0 Torr at 310.5 nm. The time scale runs from left to right with a sweep time of 0.8 μs per channel. The fraction of light absorbed is 0.0043. The plot is an average of 100 shots.

Acknowledgment

This work was supported by the Atmospheric Sciences Section of the National Science Foundation under Grant ATM-8211603 for which we are grateful.

References

- 1 J. Weaver, J. Meagher and J. Heicklen, *J. Photochem.*, **6** (1976) 111.
- 2 A. Horowitz, C. J. Kershner and J. G. Calvert, *J. Phys. Chem.*, **86** (1982) 3094.
- 3 A. Horowitz and J. G. Calvert, *J. Phys. Chem.*, **86** (1982) 3105.
- 4 H. Meyrahn, S. K. Moortgat and P. Warneck, *XVth Informal Conf. on Photochemistry, Palo Alto, CA, 1982*, Paper D-4.
- 5 R. J. Gill and G. H. Atkinson, *Chem. Phys. Lett.*, **64** (1979) 426.
- 6 R. J. Gill, W. D. Johnson and G. H. Atkinson, *Chem. Phys.*, **58** (1981) 29.
- 7 W. B. DeMore, R. T. Watson, D. M. Golden, R. F. Hampson, M. Kurylo, C. J. Howard, M. J. Molina and A. R. Ravishankara, Chemical kinetics and photochemical data for use in stratospheric modeling, *Publ. 82-57*, 1982 (Jet Propulsion Laboratory, Pasadena, CA).
- 8 H. Adachi, N. Basco and D. G. L. James, *Int. J. Chem. Kinet.*, **11** (1979) 1211.
- 9 H. Adachi, N. Basco and D. G. L. James, *Int. J. Chem. Kinet.*, **12** (1980) 949.
- 10 D. A. Parkes, D. M. Paul, C. P. Quinn and R. C. Robson, *Chem. Phys. Lett.*, **23** (1973) 425.
- 11 C. J. Hochanadel, J. A. Ghormley, J. W. Boyle and P. J. Ogren, *J. Phys. Chem.*, **81** (1977) 3.
- 12 C. J. Hochanadel, J. A. Ghormley and P. J. Ogren, *J. Chem. Phys.*, **56** (1972) 4426.
- 13 T. T. Paukert and H. S. Johnston, *J. Chem. Phys.*, **56** (1972) 2824.
- 14 R. A. Cox and J. P. Burrows, *J. Phys. Chem.*, **83** (1979) 2560.